Journal of Organometallic Chemistry, 378 (1989) 125–137
Elsevier Sequoia S.A., Lausanne – Printed in The Netherlands
JOM 20295

Synthesis of diethyl- and diisopropylamino-trifluoromethylboranes and their reactions with HF, HCl, HBr and H_2O. The crystal structure of $(CF_3)_2BN(i\text{-}Pr)_2$, revealing a very short B–N bond

D.J. Brauer, H. Bürger, F. Dörrenbach, G. Pawelke and W. Weuter

Anorganische Chemie, Fachbereich 9, Universität-Gesamthochschule, D-5600 Wuppertal (F.R.G.)

(Received June 16th, 1989)

Abstract

The novel trifluoromethyl-aminoboranes $(CF_3)(Cl)BNEt_2$ (I), $(CF_3)(Br)BNEt_2$ (II), $(CF_3)_2BNEt_2$ (III) and $(CF_3)_2BN(i\text{-}Pr)_2$ (IV) have been prepared by the reaction of Cl_2BNEt_2, Br_2BNEt_2 and $Br_2BN(i\text{-}Pr)_2$ with the trifluoromethylating agent $P(NEt_2)_3/CF_3Br$ in CH_2Cl_2. The reactions of these trifluoromethylboranes with HX (X = F, Cl, Br and OH) have been investigated, and the following 1/1 addition products obtained in high yields: $CF_3BCl_2 \cdot NHEt_2$ (V); $CF_3BBr_2 \cdot NHEt_2$ (VI); $(CF_3)_2BX \cdot NHEt_2$, X = F (VII), X = Cl (VIII), X = Br (IX), X = OH (X); $(CF_3)_2BX \cdot NH(i\text{-}Pr)_2$, X = F (XI), X = Cl (XII), X = Br (XIII). The structure of aminoborane IV was determined by an X-ray diffraction study. A strong π contribution to the B–N bond is suggested by the planarity of the C_2BNC_2 fragment and the B–N bond length, 1.37(1) Å.

Introduction

The synthesis of some trifluoromethyl derivatives of tricoordinate boron was reported in the sixties [1,2] but these compounds were never fully characterized. Recently it has been shown that such species can be stabilized by amino groups, and unambiguous access to amino-trifluoromethylboranes has been achieved by use of the novel trifluoromethylating agent $CF_3Br/(Et_2N)_3P$, (discovered by Ruppert [3]) in polar solvents. However, the yields of the isolated compounds, $CF_3B(NMe_2)_2$ (20%) and $(CF_3)_2BNMe_2$ (**B1**) (8%) [4] were unsatisfactory. We found that both incomplete trifluoromethylation of X_2BNR_2 (X = Cl, Br) to give $CF_3(X)BNR_2$ and addition of CF_3^- to give the anion $(CF_3)_3BNR_2^-$ were important side reactions which reduced the yield of the desired material. In particular the latter reaction was found to dominate if an excess of the trifluoromethylating agent was employed, and

0022-328X/89/$03.50

the tetracoordinate borane-amine $(CF_3)_3B \cdot NHEt_2$ has been obtained in 32% yield by the reaction of Cl_2BNEt_2 with $(Me_2N)_2C{=}C(NMe_2)_2/CF_3I$ in CH_2Cl_2 [5].

It therefore seemed of interest to investigate the influence of the halogen and that of the organic groups attached to nitrogen on the course of the synthesis, and we report here on the trifluoromethylation of Cl_2BNEt_2, Br_2BNEt_2 and $Br_2BN(i\text{-}Pr)_2$ by the reagent $CF_3Br/P(Et_2N)_3$.

The reactions of $(CF_3)_2BNMe_2$ with HX, X = F, Cl, Br and OH, were shown to proceed with retention of the B–N and F_3C–B bonds to form 1/1 borane-amine adducts $(CF_3)_2B(X) \cdot NHMe_2$, whereas, depending on X, $CF_3B(NMe_2)_2$ gave $CF_3BF_2 \cdot NHMe_2$ with HF but boronium salts $CF_3B(X)(NHMe_2)_2{}^+ X^-$ with X = Cl and Br [6]. Thus one of the aspects of the present study was an examination of the reactions of the homologues with HX with the aim of assessing the stabilities of the $B\text{–}CF_3$ and B–N bonds towards protic reagents.

The structure of **B1** has been investigated by gas phase electron diffraction and shown to involve a short B–N bond, 1.425(18) Å, and a supposedly planar C_2BNC_2 skeleton [7]. On the other hand, a lengthening of the B–C bond, compared with that in $(CH_3)_3B$ was indicated, and in order to confirm these observations with greater reliability, we looked for a crystalline material suitable for a single crystal X-ray study; $(CF_3)_2BN(i\text{-}Pr)_2$ was found to be satisfactory and we report here on its preparation and crystal structure.

Results

Trifluoromethylation of aminodihalogenoboranes

The course of the trifluoromethylation reaction was monitored by ^{19}F NMR spectroscopy, the multiplicity of the ^{13}C satellites being of diagnostic value. In this way we observed successive formation of three products (eq. 1–3)

$$(Et_2N)_3P + CF_3Br + X_2BNR_2 \rightarrow \underset{(\mathbf{A})}{CF_3(X)BNR_2} + [(Et_2N)_3PX]^+ Br^- \qquad (1)$$

$$(Et_2N)_3P + CF_3Br + CF_3(X)BNR_2 \rightarrow \underset{(\mathbf{B})}{(CF_3)_2BNR_2} + [(Et_2N)_3PX]^+ Br^- \qquad (2)$$

$$(Et_2N)_3P + CF_3Br + (CF_3)_2BNR_2 \rightarrow \underset{(\mathbf{C})}{(CF_3)_3BNR_2{}^-} + [(Et_2N)_3PBr]^+ \qquad (3)$$

(X = Cl, Br; R = Me, Et, i-Pr)

The relative concentrations of products **A**, **B** and **C** for X = Br and R = Et depend on the molar ratio of the trifluoromethylating reagent to X_2BNR_2, as shown in Fig. 1. Compound **A** is formed first and predominates until the ratio exceeds 1.5. The yield of compound **B** reaches its maximum at a ratio of ca. 2, but never exceeds ca. 45%. The only product which is formed selectively, at a ratio $\geqslant 3$, is the anion **C**, which will be reported elsewhere.

It is obvious that the yield of bis(trifluoromethyl)diethylaminoborane cannot be higher than ~ 40%, and owing to decomposition and loss upon work-up the actual yield is only ~ 20%. It is even smaller, ~ 17%, for $(CF_3)_2BNMe_2$ (**B1**), whereas, owing to the effect of steric hindrance on the reaction shown in eq. 3, $(CF_3)_2BN$(i-

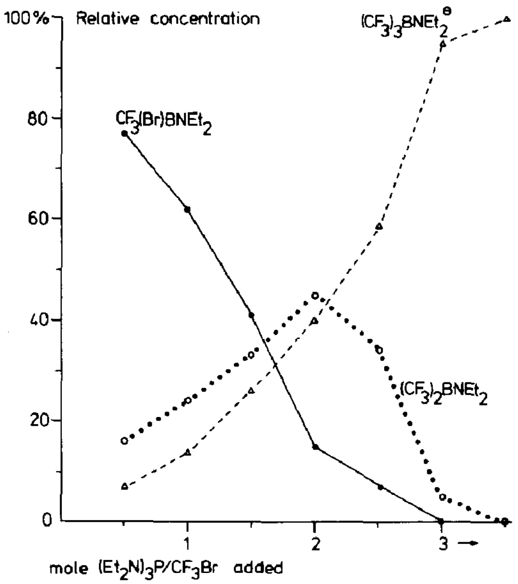

Fig. 1. Relative formation of II, III and $(CF_3)_3BNEt_2^-$ in dependence of $(Et_2N)_3P/CF_3Br$ reagent added to Et_2NBBr_2.

$Pr)_2$ is typically obtained in a yield of ~ 35%. Change of X from Cl to Br has no significant effect on the yield.

The novel non-ionic trifluoromethyldialkylaminoboranes I–IV were isolated under the appropriate conditions: $CF_3(Cl)BNEt_2$ (I), $CF_3(Br)BNEt_2$ (II), $(CF_3)_2BNEt_2$ (III), and $(CF_3)_2BN(i\text{-}Pr)_2$ (IV). Their physical properties are summarized in Table 1. They are moisture-sensitive, but are stable at room temperature, although storage in sealed ampoules at − 78 °C is recommended. Compounds I and II are thermally more stable than III, which was shown to withstand heating at 80 °C for 4 h. Compounds I–IV showed no tendency to oligomerize.

Formation of 1/1 adducts with HX

The aminoboranes I–IV react in etheral solution with hydrogen halides HX (X = F, Cl, and Br) or H_2O to give, in yields of 80–98%, the corresponding 1/1 adducts V–XIII according to eq. 4 and 5:

$$CF_3(X)BNR_2 + HX \rightarrow CF_3(X)_2B \cdot NHR_2 \quad (4)$$

$$(CF_3)_2BNR_2 + HX \rightarrow (CF_3)_2(X)B \cdot NHR_2 \quad (5)$$

$CF_3(Cl_2)B \cdot NHEt_2$ (V), $CF_3(Br_2)B \cdot NHEt_2$ (VI), $(CF_3)_2FB \cdot NHEt_2$ (VII), $(CF_3)_2ClB \cdot NHEt_2$ (VIII), $(CF_3)_2BrB \cdot NHEt_2$ (IX), $(CF_3)_2BOH \cdot NHEt_2$ (X), $(CF_3)_2FB \cdot NH(i\text{-}Pr)_2$ (XI), $(CF_3)_2ClB \cdot NH(i\text{-}Pr)_2$ (XII), and $(CF_3)_2BrB \cdot NH(i\text{-}Pr)_2$ (XIII).

In the case of V–VII, possible halogen-exchange side reactions were avoided by using HX with the same X as that attached to the boron atom. The physical properties of the complexes V–XIII, which can be sublimed (or, for VII, distilled), are set out in Table 2. The boron–halogen bonds of V, VI, VIII, IX, XII and XIII are slowly hydrolyzed in moist air, without cleavage of B–CF_3 bonds, to yield trifluoromethyl(hydroxy)borane derivatives as the initial products, of which the

Table 1

Physical properties and NMR spectral data for trifluoromethyldialkylaminoboranes I–IV (δ in ppm, J in Hz)

		I	II	III	IV
B.p.	(°C/Torr)	52/30	64/30	55/33	
M.p.	(°C)				44
^1H [a]	$\delta(CH_3)$	1.21	1.21	1.2	1.3
		1.19	1.19		
	$\delta(CH_2)$	3.34	3.36	3.4	
		3.36	3.40		
	$\delta(CH)$				4.0
	$^3J(HH)$	7.1	7.1	7.1	6.8
		7.2	7.2		
^{13}C [b]	$\delta(CH_3)$	14.1	14.3	15.4	22.5
		15.1	15.4		
	$\delta(CH_2)$	43.5	44.2	45.2	
		44.5	46.6		
	$\delta(CH)$				51.1
	$^4J(FC)$	1.8	2.2		
^{19}F [c]	$\delta(CF_3)$	−64.6	−63.5	−63.4	−61.0
^{11}B [d]	$\delta(B)$	29.9	30.2	27.1	26.2

[a] I–III in $CDCl_3$, 250.13 MHz, int. std. $CHCl_3$ 7.27 ppm, IV in CD_2Cl_2, 90 MHz, int. std. TMS. [b] I–III in $CDCl_3$, 62.9 MHz, int. std. $CDCl_3$ 77.0 ppm, IV in CD_2Cl_2, 20 MHz, int. std. CD_2Cl_2 53.1 ppm. [c] I–IV 84.67 MHz, solvent and int. std. $CFCl_3$. [d] I–IV in $CDCl_3$, 25.52 MHz, ext. std. $F_3B \cdot OEt_2$.

hydroxide X was isolated. Adducts with HF and presumably also the others with H_2O are resistant to hydrolysis at ambient temperatures.

NMR spectra

The constitutions of compounds I–XIII were established by ^1H, ^{19}F, ^{13}C and ^{11}B NMR spectroscopy. Chemical shifts and coupling constants are set out in Tables 1 and 2. As expected for a rigid $C(X)BNC_2$ skeleton, two non-equivalent C_2H_5 groups are observed in the ^1H and ^{13}C NMR spectra of I and II. The interaction with a CF_3 group is evident from the quartet observed for the methylene ^{13}C resonance appearing at higher field. This C atom is assigned as *cis* to the CF_3 group for two reasons. First, long range $^{19}F \ldots {}^{13}C$ couplings are usually only observed if the distance between both nuclei is short [8]. Second, substituted ethanes of the general formula $C^3{\setminus}C{=}C{<}^{C^1}_{C^2}$ usually reveal an upfield shift of C^1 with respect to C^2 [8]. In the tetracoordinate species V to IX, a small $^4J(CF)$ coupling constant of 1.5 Hz was also found.

Only broad ^{19}F and ^{11}B signals are observed for the tricoordinate boron derivatives I–IV, but 1/1/1/1 quartets are given by the tetracoordinate adducts, with $^2J(FB)$ 30–40 Hz. In this case the multiplicity of the ^{11}B signals is indicative of the number of CF_3 groups bonded to the tetracoordinate B atom.

In general, chemical shifts and coupling constants are in line with previous observations [4,6].

Mass and vibrational spectra

Owing to the ready loss of CF_2, the mass spectra of I–XIII are not specific, and only for I, II and VI could the M^+ peaks (which show the expected Cl, Br and B

Table 2

Physical properties and NMR spectral data for compounds V–XIII (δ in ppm, J in Hz)

		V	VI	VII	VIII	IX	X	XI	XII	XIII
M.p.	(°C)	75	108		103	129	96 (dec)	73	97	128
B.p.	(°C/Torr)			63–64/3						
^1H [a]	$\delta(CH_3)$	1.42	1.46	1.36	1.43	1.45	1.34	1.5	1.5	1.5
	$\delta(CH_2)$	3.64	3.86	3.41	3.71	3.79	3.56			
	$\delta(CH_2')$	3.04	3.10	2.92	3.01	3.04	2.76			
	$\delta(CH)$							3.8	4.0	4.1
	$\delta(NH)$	3.4	3.5	3.3	3.3	3.4	3.1	~3.5	~3.5	~3.5
	$^3J(HH)$	7.3	7.3	7.3	7.3	7.3	7.3	6.8	6.8	6.8
	$^2J(HH')$	13.5	13.6	13.7	13.7	13.6	13.7			
	$^3J(H(N)H)$	2.2	2.0	2.3	2.1	2.0	1.4			
	$^3J(H(N)H')$	6.7	6.7	6.7	7.0	7.0	7.8			
^{13}C [b]	$\delta(CH_3)$	12.9	13.5	13.4	13.8	13.9	14.1	20.4	20.6	20.3
	$\delta(CH_3')$							20.5	21.0	21.5
	$\delta(CH_2)$	46.3	48.5	45.0	47.5	48.5	45.4			
	$\delta(CH)$							51.0	54.0	55.2
	$^4J(CF)$	1.5	1.5	1.5	1.7	1.7	–			
^{19}F [c]	$\delta(CF_3)$	−70.9	−68.6	−70.3	−66.9	−65.3	−67.5	−70.2	−66.3	−64.4
	$\delta(BF)$			−201.7				−196.8		
	$^2J(BF)$	38.4	40.6	32.2	35.0	36.7	–	32.5	33.9	36.1
	$^1J(BF)$			64.9				67.0		
^{11}B [d]	$\delta(B)$	−1.4	−2.3	−2.4	−4.3	−5.9	−4.3	−2.1	−5.5	−6.0

[a] V–X in $CDCl_3$, 250.13 MHz, int. std. $CHCl_3$ 7.27 ppm, XI–XIII in CD_2Cl_2, 90 MHz, int. std. TMS. [b] V–X in $CDCl_3$, 62.9 MHz, int. std. $CDCl_3$ 77.0 ppm, XI–XIII in CD_2Cl_2, 20 MHz, int. std. CD_2Cl_2 53.1 ppm. [c] 84.67 MHz, solvent and int. std. $CFCl_3$. [d] In $CDCl_3$, 25.52 MHz, ext. std. $BF_3 \cdot OEt_2$.

Table 3

Selected IR/Raman bands (cm^{-1}) for compounds I–XIII

Nr.	ν(OH) (IR)	ν(NH) (IR)	$\nu(^{11}B{=}N)$ (IR)	$\nu(CF_3)$ (IR)	$\delta_s(CF_3)$ (Raman)/(IR)	ν(BX) (Raman)
I			1521m	1135vs/1087vs	708vs/–	387m
II			1518m	1134vs/1085vs	700vs/–	310vs
III			1547m	1153vs/1107vs	725vs/692m	
IV			1534w	1156s/1102vs	719s/688m	
V		3200m		1104vs/1078vs	688s/–	377s
VI		3200m		1100vs/1073vs	676m/–	268s
VII		3246m		1104vs/1056vs/1038vs	722vs/689vs	
VIII		3244m		1101vs/1070s/1051s	723s/681s	
IX		3243m		1102vs/1073s/1051s	719s/680s	
X	3665w	3278m		1098vs/1076vs/1059s	721m/692s	
XI		3243m		1128s/1107s/1085s	720s/697vs	
XII		3240w		1121s/1104s/1082s	718s/688m	
XIII		3246w		1112vs/1090s/1078s	717m/687m	

isotopic patterns) be observed, and then only with low intensity. Typical base peak ions for the NEt_2 derivatives are $F_2BNC_3H_7^+$ and $FClBNC_3H_7^+$, while $F_2BNC_5H_{11}^+$ is the base ion in the mass spectrum of IV. An intact $BNHR_2$ entity is common to the ions formed in the first fragmentation steps of the 1/1 adducts V–XIII.

The vibrational spectra are too complex to be analyzed fully but some diagnostic vibrations were detected in the infrared and Raman spectra, data for which are listed in Table 3. Among these are the NH and OH stretching vibrations of V–XIII at 3200 and 3665 cm^{-2}, respectively. For I–IV the ν(BN) vibration at 1520–1550 cm^{-1} (^{11}B) is identified by its 20–30 cm^{-1} isotopic shift. This vibration may be compared with that found in **B1**, 1570 cm^{-1} [7], which, however, does not display the full $^{10/11}B$ isotope shift calculated by a normal coordinate analysis (49 cm^{-1}) because of coupling with inner vibrations of the NMe_2 group. A similar shortfall in the $^{10/11}B$ isotope shift is found for I–IV. Nevertheless the wavenumbers of the BN stretching vibration suggest an increased bond strength. In the complexes V–XIII the BN stretching vibration, due to weakening of the BN bond, is shifted to low wavenumbers and buried in the congested region of the CF_3 and NR_2 skeletal stretching and HCH bending vibrations. The CF_3 stretching vibrations are associated with strong infrared absorptions in the 1040–1160 cm^{-1} region. The symmetric CF_3 bending vibration near 700 cm^{-1}, usually associated with a strong Raman line, is characteristically doubled whenever two CF_3 groups are bonded to the B atom. The BCl and BBr vibrations are associated with Raman lines, and are expected to be mixed with other vibrations.

X-ray structural analysis

Crystals of $(CF_3)_2BN(i\text{-}Pr)_2$ are volatile, easily deformed, and extremely sensitive to air, and most specimens examined gave unsatisfactory reflections. A Weissenberg study indicated that the crystals are monoclinic, possible space groups being $P2_1$ and $P2_1/m$. Further X-ray measurements were made with a Siemens AED-1 diffractometer employing Ni filtered Cu-K_α-radiation (λ 1.54184 Å). Crystal data are given in Table 4; the lattice constants were determined from 56 Bragg angles ($28° < \theta < 36°$).

The first data set (hkl, $\bar{h}kl$; $\theta \leq 50°$) was obtained with a crystal manually mounted in a glass capillary under argon. The crystal, which gave good ω profiles, showed signs of decomposition during data collection (the three standards lost 16% of their initial intensity), and hourly recentering was necessary in order to keep the peaks in the middle of the θ–2θ scan range. Subsequent data reduction and application of direct methods, with space group $P2_1/m$ indicated by the distribution of the E's, led to the location of the nonhydrogen atoms. Least-squares refinement of the structure with nonhydrogen atoms anisotropic and hydrogen atoms idealized (C–H 0.95 Å) converged with $R = 0.120$ for the 542 observed reflections ($F_0 \geqq 4\sigma\,(F_0)$).

In order to improve the accuracy of the structural determination, data were collected from a second crystal. This irregularly-shaped specimen was obtained by repeated sublimation (30 °C) of material which had been sealed in a glass capillary under argon. The crystal gave sharp and symmetrical ω-scans, and a hemisphere of data was collected ($\theta \leq 70°$). During the measurement the orientation was stable, and the intensities of the three standard reflections fell by only 4%. Equivalents were merged, and refinement of the previously described model with an extinction correction, $F_c' = F_c\,(1 - xF_c^2/\sin\theta)$, converged with $R = 0.136$. A difference Fourier map revealed peaks (0.36 to 0.72 e/Å^3) suggesting alternative positions ("A") for C(3), C(5) and the fluorine atoms. These alternative atoms were refined isotropically with occupancy $1 - \alpha$ while their counterparts and the idealized hydrogen atoms were assigned an occupancy of α. Refinement of this disorder model converged with $R = 0.088$, $\alpha = 0.826(7)$ and $x = 6.1(6) \times 10^{-6}$. Details of the data collection with

Table 4

Details of the crystal structure analysis

Formula	$(CF_3)_2BN(i\text{-}Pr)_2$
M_r	249.01
Space group	$P2_1/m$
a	8.1824(5) Å
b	10.400(1) Å
c	7.6646(6) Å
β	111.197(5)°
Z	2
D_c	1.360 g/cm^3
T	23 °C
Measured reflections	2527
Unique reflections	1168
Observed ($F_0 \geqq 4\sigma(F_0)$)	1070
Monitor correction	1.016–0.963
μ(Cu-K_α)	12.85 cm^{-1}
Parameters	108
R [a]	0.088/0.092 [b]
wR	0.121/0.122
ρ(e/Å^3) [c]	0.31 to −0.23

[a] $R = \Sigma\Delta/\Sigma|F_0|$, $wR = [\Sigma w\Delta^2/\Sigma w|F_0|^2]^{1/2}$, $\Delta = ||F_0| - |F_c||$, $w^{-1} = \sigma^2(F_0)$. [b] First value for observed reflections only, second value for all reflections. [c] Densities in final difference Fourier map.

Table 5

Positional and equivalent isotropic temperature factors [a] for IV

Atom	x	y	z	U
B	−0.0148(5)	0.2500	0.3659(7)	0.070(2)
N	0.1603(4)	0.2500	0.3966(5)	0.069(1)
C(1)	−0.1713(6)	0.2500	0.1636(7)	0.100(2)
C(2)	−0.0889(7)	0.2500	0.529(1)	0.113(3)
C(3)	0.2858(6)	0.2500	0.6040(8)	0.079(2)
C(4)	0.3908(6)	0.3705(4)	0.6473(6)	0.122(2)
C(5)	0.2533(7)	0.2500	0.2656(9)	0.081(2)
C(6)	0.2324(6)	0.3716(4)	0.1559(5)	0.115(2)
F(1)	−0.1304(5)	0.2500	0.0094(5)	0.168(3)
F(2)	−0.2741(5)	0.3500(4)	0.1389(5)	0.157(2)
F(3)	−0.2709(5)	0.2500	0.4605(7)	0.183(4)
F(4)	−0.0508(5)	0.3528(4)	0.6364(5)	0.149(2)
F(1A)	−0.330(3)	0.2500	0.233(4)	0.15(1)
F(2A)	−0.201(3)	0.352(2)	0.093(3)	0.117(6)
F(3A)	0.074(3)	0.2500	0.728(4)	0.152(9)
F(4A)	−0.180(4)	0.336(3)	0.535(4)	0.175(9)
C(3A)	0.329(3)	0.2500	0.523(4)	0.070(7)
C(5A)	0.167(3)	0.2500	0.172(3)	0.056(5)

[a] $U = \frac{1}{3}\Sigma_i\Sigma_j U_{ij}\bar{a}_i \cdot \bar{a}_j a_i^\star a_j^\star$.

the second crystal and refinement are given in Table 4, and coordinates of the nonhydrogen atoms are listed in Table 5. The program SHELX-76 [9] was used to solve and refine the structure, ORTEP-II [10] was used for the drawing (Fig. 2) and local routines were used for coordinate transformations [11].

Description and discussion of the crystal structure

In the structure of IV, the atoms of a $(CF)_2BN(CH)_2$ fragment are constrained to lie in the crystallographic mirror plane. The possibility of lower symmetry was

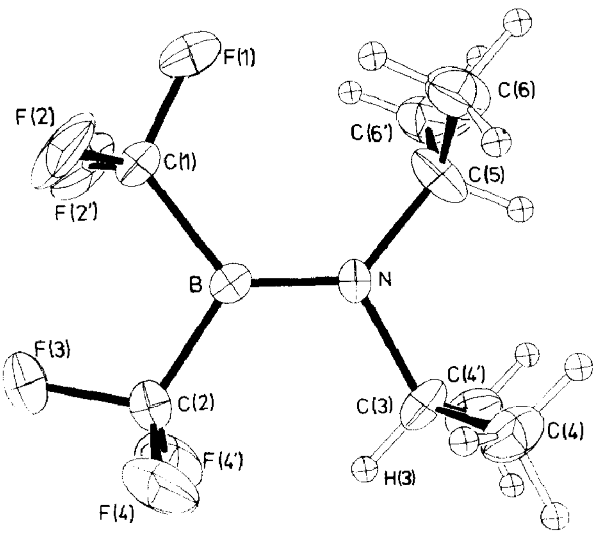

Fig. 2. A perspective drawing of the major orientation of IV employing 20% probability thermal ellipsoids.

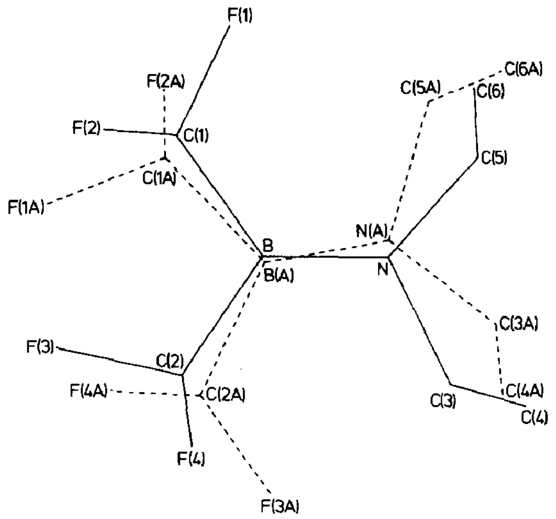

Fig. 3. A projection showing the relationship between the disordered atoms of IV, mirror-related positions being omitted.

considered; that is, the molecule was rotated out of the plane and then refined in space groups ($P2_1$, $P\bar{1}$) which have no mirror planes. Since the latter refinements did not lead to convincingly non-planar structures, the $P2_1/m$ model is to be preferred. The large values for the discrepancy indices are attributed to inadequacies in the disorder model.

The highest conceivable symmetry for IV is C_{2v}, but repulsions between the CF_3 and i-Pr substituents can best be relieved with retention of a planar C_2BNC_2 fragment by lowering the symmetry. For example, C_2 symmetry was found by gas phase electron diffraction for the sterically less-crowded species **B1**, the symmetry being reduced from C_{2v} by rotations about the B–C and N–Me bonds [7]. Figure 2 shows that IV does not possess a twofold axis. Such symmetry would be incompatible with the perfect gearing exhibited by the substituents; that is, the in-plane protrusion of each CF_3 and i-Pr group is directed towards an in-plane hollow of a neighbour.

The disorder found with the second data set was also evident in a difference Fourier map derived from the first data set. At that point, however, the "spurious" peaks were attributed to the low quality of the data.

The disorder in IV may be described in terms of the occupancy of the molecular site by molecules in two different orientations (Fig. 3). Examination of interatomic distances indicates that the atoms of the F(1), F(3), C(3), C(5) fragment correspond in a one-to-one fashion to those of the F(3A), F(1A), C(5A), C(3A) entity. While a simple coordinate transformation fits the atoms of the former fragment to those of the latter to within 0.02 Å, the coordinates x_A thus generated for the B(A), N(A), C(1A), C(2A), C(4A) and C(6A) atoms lie up to 0.4 Å from their counterparts with coordinates x. Such pairs are too close to be resolved into individual atoms, and least-squares refinement would yield weighted average positions $\bar{x}$. The coordinates x of occupancy α may be derived in an iterative fashion from $\bar{x}$ and x_A using eq. 6. The new x coordinates replace $\bar{x}$ when

$$x = (\bar{x} - x_A + \alpha x_A)/\alpha \quad (6)$$

Table 6

Deconvoluted coordinates ($\times 10^4$)

B	−160	2500	3638	B(A)	−92	2500	3758
N	1617	2500	4039	N(A)	1536	2500	3623
C(1)	−1689	2500	1561	C(1A)	−1828	2500	1990
C(2)	−969	2500	5207	C(2A)	−510	2500	5683
C(4)	3972	3702	6513	C(4A)	3607	3719	6283
C(6)	2268	3719	1590	C(6A)	2590	3702	1413

generating x_A coordinates in subsequent cycles. After four cycles the procedure was terminated, since no atom shifted by more than 0.0005 Å. The deconvoluted x and x_A coordinates are listed in Table 6.

Comparison is made in Table 7 of bond lengths calculated with weighted average and deconvoluted coordinates. The latter give much more reasonable distances for the low-occupancy orientation, and the good agreement between the two deconvoluted structures confirms the assumption that overlapping molecules have similar structures. Since the positional parameters for the low occupancy atoms are less reliable, further discussion relates only to the major orientation. For the latter a comparison of the bond angles calculated with averaged and deconvoluted coordinates is given in Table 8. The superiority of the deconvoluted values is suggested by the smaller spread of the calculated F–C–F angles (2.3° instead of 6.3°), and reference will be made to the deconvoluted structure below. The standard deviations are estimated to be 0.01 Å for the B–N, B–C and N–C bond lengths, 0.03 Å for the C–F and C–C bonds, and 1° for the bond angles.

The two steric interactions which straddle the B–N bond are different. In one case the C(1)–F(1) bond is projected towards an opening in the C(6)–C(5)–C(6′) angle, and in the other the C(3)–H(3) bond is directed towards the hollow of the F(4)–C(2)–F(4′) angle. The former situation appears to be sterically more demanding; that is, the N–B–C(1) and B–N–C(5) bond angles are 4(1) and 7(1)° larger, respectively, than their N–B–C(2) and B–N–C(3) counterparts. Furthermore, both

Table 7

Comparison of distances (Å) between averaged and deconvoluted atomic positions

B–N	1.365(5) [a]	1.373 [b]			
B–C(1)	1.615(6)	1.631			
B–C(2)	1.574(8)	1.568			
C(1)–F(1)	1.340(7)	1.273	C(1)–F(1A)	1.57(3) [a]	1.32 [c]
C(1)–F(2)	1.308(4)	1.326	C(1)–F(2A)	1.18(2)	1.32
C(2)–F(3)	1.389(7)	1.328	C(2)–F(3A)	1.62(3)	1.28
C(2)–F(4)	1.316(5)	1.353	C(2)–F(4A)	1.18(2)	1.34
N–C(3)	1.549(6)	1.502	N–C(3A)	1.37(2)	1.51
N–C(5)	1.463(6)	1.503	N–C(5A)	1.74(2)	1.50
C(3)–C(4)	1.488(5)	1.512	C(3A)–C(4)	1.55(2)	1.48
C(5)–C(6)	1.494(5)	1.481	C(5A)–C(6)	1.40(1)	1.52

[a] No deconvoluted coordinates were used to calculate the distances in this column. [b] Deconvoluted coordinates of the high occupancy positions were used in calculating values for this column. [c] Deconvoluted coordinates of the low occupancy positions were used to determine the bond distances in this column.

Table 8

Selected bond angles for the refined and deconvoluted models [a]

C(1)–B–C(2)	111.3(4)	111.2	B–C(2)–F(4)	115.1(3)	114.0
C(1)–B–N	125.7(4)	126.5	F(1)–C(1)–F(2)	103.0(4)	105.7
C(2)–B–N	123.0(4)	122.4	F(2)–C(1)–F(2′) [b]	105.4(6)	103.4
C(3)–N–C(5)	112.8(3)	113.2	F(3)–C(2)–F(4)	102.4(3)	103.7
B–N–C(3)	116.2(4)	119.9	F(4)–C(2)–F(4′)	108.7(6)	104.5
B–N–C(5)	131.0(4)	126.9	N–C(3)–C(4)	110.1(3)	111.8
B–C(1)–F(1)	118.9(4)	121.0	N–C(5)–C(6)	113.8(3)	112.2
B–C(1)–F(2)	112.6(3)	109.8	C(4)–C(3)–C(4′)	114.8(5)	111.5
B–C(2)–F(3)	111.6(5)	115.5	C(6)–C(5)–C(6′)	115.7(5)	117.7

[a] The first value was calculated from the coordinates in Table 2 while deconvoluted coordinates of high occupancy for the B, N, C(1), C(2), C(4) and C(6) atoms were used to calculate the second angle. [b] Symmetry code: $x', y', z' = x, 0.5-y, z$.

the B–C–F(1) and C(6)–C(5)–C(6′) bond angles are markedly large (121(1) and 118(1)°, respectively). Perhaps steric interactions cause the B–C(1) bond (1.63(1) Å) to be longer than B–C(2) (1.57(1) Å), but the difference seems somewhat exaggerated. The B–C bond distances in **B1** were found to have an intermediate value, 1.623(4) Å.

Steric forces are probably also responsible for the fact that the C(1)–B–C(2) bond angle in IV (111(1)°) is much smaller than that in **B1** (122.2(5)°). While no such large difference is seen in the C–N–C angles (cf. 113(1)° in IV and 111(1)° in **B1**), the N–C bond distances in IV (1.50(1) Å) are significantly longer than those in **B1** (1.453(2) Å). The longer N–C distances in IV are accompanied by a B–N bond length (1.37(1) Å) significantly shorter than that in **B1** (1.425(6) Å).

An alternative molecular deformation which would relieve steric repulsions in IV involves a twisting about the B–N bond, but this would have to be at the expense of $N(p\pi) \rightarrow B(p\pi)$ bonding. In the solid state, however, the molecule reduces steric interactions by adopting a novel geared conformation and retains a planar C_2BNC_2 framework. The structure is strongly stabilized by π bonding, the distance between the three-coordinate B and N atoms being the shortest on record (cf. 1.379(6) Å in Cl_2BNMe_2 [12]).

Experimental

Diisopropylaminobis(trifluoromethyl)borane (IV). At −78°C, 150 g of CF_3Br were condensed into a solution of 200 mmol (54.2 g) of $Br_2BN(i\text{-}Pr)_2$ in 200 ml of CH_2Cl_2, and 410 mmol of $(Et_2N)_3P$ were added dropwise during 1.5 h. The mixture was warmed to room temperature and stirred for 6 h. The solvent was removed and IV trapped in vacuo at −78°C as the temperature of the mixture was raised to 90°C. Compound IV was purified by repeated vacuum sublimation at room temperature, and obtained in 35% yield. For elemental analyses see Table 9.

Chloro(diethylamino)(trifluoromethyl)borane (I), bromo(diethylamino)(trifluoromethyl)borane (II) and (diethylamino)bis(trifluoromethyl)borane (III). These were similarly prepared from Cl_2BNEt_2 and Br_2BNEt_2 and purified by repeated distillation in vacuo through a slit-tube column (Fischer; 50 theoretical plates). Typical yields were as follows: ratio $Cl_2BNEt_2/(Et_2N)_3P$ 1/1.2 10% I, $Br_2BNEt_2/(Et_2N)_3P$ 1/1.2 10% II, and $Br_2BNEt_2/(Et_2N)_3P$ 1/2.2 20% III.

Table 9

Elemental analyses

Compound	Formula	Analyses (Found(calc.) (%))			
		C	H	Br/Cl	F
I	$C_5H_{10}BClF_3N$	32.0 (32.05)	5.4 (5.38)	20.1 (18.92)	29.4 (30.41)
II	$C_5H_{10}BBrF_3N$	26.4 (25.90)	4.5 (4.35)	33.4 (34.46)	24.7 (24.58)
III	$C_6H_{10}BF_6N$	32.8 (32.62)	4.6 (4.89)		51.4 (51.59)
IV	$C_8H_{14}BF_6N$	38.5 (38.59)	5.9 (5.67)		45.9 (45.78)
V	$C_5H_{11}BCl_2F_3N$	26.8 (26.83)	5.0 (4.95)	32.2 (31.67)	25.1 (25.46)
VI	$C_5H_{11}BBr_2F_3N$	20.7 (19.20)	3.9 (3.55)	48.3 (51.10)	18.6 (18.22)
VII	$C_6H_{11}BF_7N$	30.1 (29.91)	4.6 (4.60)		54.9 (55.19)
VIII	$C_6H_{11}BClF_6N$	28.1 (28.00)	4.5 (4.31)	14.0 (13.77)	44.5 (44.28)
IX	$C_6H_{11}BBrF_6N$	24.1 (23.87)	3.7 (3.67)	26.7 (26.47)	37.4 (37.76)
X	$C_6H_{12}BF_6NO$	31.2 (30.16)	4.9 (5.06)		47.4 (47.70)
XI	$C_8H_{15}BF_7N$	36.1 (35.72)	5.5 (5.62)		48.5 (49.43)
XII	$C_8H_{15}BClF_6N$	34.3 (33.66)	5.2 (5.30)	13.2 (12.42)	38.6 (39.93)
XIII	$C_8H_{15}BBrF_6N$	29.6 (29.12)	4.4 (4.58)	24.5 (24.22)	32.9 (34.55)

Fluorobis(trifluoromethyl)borane · diethylamine (VII) and fluorobis(trifluoromethyl) borane · diisopropylamine (XI). An excess of anhydrous HF was condensed into a solution of 10 mmol of III (or IV) in 5 ml dry ether in a stainless steel cylinder at − 196 °C. The mixture was warmed to room temperature and kept there for 6 h. After removal of Et_2O and HF, VII (or XI) was obtained by distillation (or sublimation) in vacuo in 30% yield.

Dichloro(trifluoromethyl)borane · diethylamine (V), dibromo(trifluoromethyl)borane · diethylamine (VI), chlorobis(trifluoromethyl)borane · diethylamine (VIII), bromobis-(trifluoromethyl)borane · diethylamine (IX), chlorobis(trifluoromethyl)borane · diisopropylamine (XII) and bromobis(trifluoromethyl)borane · diisopropylamine (XIII). A solution of 10 mmol of the aminoborane in 10 ml dry ether was treated at − 78 °C with an excess of HCl or HBr. The mixture was warmed to room temperature and, after removal of volatile material, the products were purified by sublimation in vacuo. Yields 80–98%.

Hydroxybis(trifluoromethyl)borane · diethylamine (X). Water (0.4 ml) was added at − 78 °C to a solution of 10 mmol (2.2 g) of III in 20 ml of CH_2Cl_2. The mixture was stirred and warmed to room temperature. After removal of the solvent and unchanged H_2O, compound X was purified by sublimation in vacuo and isolated in 80% yield.

Acknowledgements

We thank the Fonds der Chemie for financial support.

References

1 T.D. Parson, J.M. Self and L.H. Schaad, J. Am. Chem. Soc., 89 (1967) 3446.
2 T.D. Parson, E.D. Baker, A.B. Burg and G.L. Juvinall, J. Am. Chem. Soc., 83 (1961) 250.
3 I. Ruppert, K. Schlich and W. Volbach, Tetrahedron Lett., 25 (1984) 2195.
4 H. Bürger, M. Grunwald and G. Pawelke, J. Fluor. Chem., 31 (1986) 89.
5 G. Pawelke, J. Fluor. Chem., 42 (1989) 429.
6 D.J. Brauer, H. Bürger, G. Pawelke, W. Weuter and J. Wilke, J. Organomet. Chem., 329 (1987) 293.
7 R. Hausser-Wallis, H. Oberhammer, H. Bürger and G. Pawelke, J. Chem. Soc., Dalton Trans., (1987) 1839.
8 H.O. Kalinowski, S. Berger and S. Braun, ^{13}C-NMR-Spektroskopie, Thieme, Stuttgart/New York, 1984.
9 G.M. Sheldrick, SHELX-76: Program for crystal structure determination, University of Cambridge, England, 1976.
10 C.K. Johnson, ORTEP-II: Report ORNL-5138, Oak Ridge National Laboratory, Tennessee, 1976.
11 Additional crystallographic details may be obtained from Fachinformationszentrum Energie-Physik-Mathematik GmbH, D-7514 Eggenstein-Leopoldshafen 2, by quoting the deposit number CSD 54044, the authors and the literature reference.
12 F.B. Clippard, Jr., and L.S. Bartell, Inorg. Chem., 9 (1970) 2439.